Proceedings of the 17th World Congress
The International Federation of Automatic Control
Seoul, Korea, July 6-11, 2008

Integrated Autopilot and Guidance for Dual Control Missiles Using Higher Order Sliding Mode Control and Observers

C. H. Tournes*. Y. B. Shtessel**

** Davidson Technologies, Huntsville, AL, 35899, USA*
(Tel: 256-922-0720; e-mail: christiantournes@davidson-tech.com)
*** University of Alabama in Huntsville, Huntsville, AL, 35899, USA (e-mail: shtessel@ece.uah.edu)*

Abstract: An integrated Autopilot-and Guidance Algorithm is developed using Higher Order Sliding Mode Control, for interceptors steered by combination of aerodynamic lift, sustainer thrust and center of gravity divert thrusters. A smooth HOSM guidance generates flight path trajectory angular rates and attitude rate commands. The attitude rate maneuvers are aimed at producing desired aerodynamic lift and / or orienting sustainer thrust. The lateral acceleration created by the attitude maneuver is treated as a "cooperative" disturbance and accounted for by the trajectory control. SOSM autopilot design is based on nonlinear dynamic sliding manifold. Proposed algorithm also includes seeker tracker, bore sight stabilization and estimation of target lateral acceleration. The algorithm is tested using computer simulations against a ballistic maneuvering target.

1. INTRODUCTION

To cope with increasingly larger ballistic target maneuvering capabilities a future missile interceptor may be steered by possible combination of aerodynamic-lift, sustainer-thrust and center-of-gravity divert thrusters. This poses serious Guidance Navigation and Control (Garnell and East, 1977; Zarchan, 1998) challenges and calls for the integrated design of all interceptor modules: sensor information processing and data estimation, a homing guidance law, and autopilot.

The goal of this work is in developing an integrated robust guidance and control technology for dual controlled missile interceptors via Higher Order Sliding Mode Control and Observers in order to achieve the hit-to-kill accuracy against targets performing high-amplitude evasive maneuvers.

Traditional sliding mode control (SMC) (Edwards and Spurgeon; 1998) is used for developing a guidance laws for missile interceptors that is robust to target maneuvers (Idan, et. al, 2007; Moon and Kim, 2000; Shkolnikov, et. al., 2001). The main problem is in necessity of smoothing high frequency switching control function by a price of loosing robustness.

Higher order sliding mode control (HOSM) (Levant, 2003) mitigates the problems associated with SMC, i.e. HOSM is applicable to the systems with arbitrary relative degree and continuous/smooth control functions can be designed while the robustness is retained. Development of the *smooth* robust guidance law to target maneuvers (Shtessel et. al., 2005, 2007) is essential for effective following this law by the autopilot and also for integrating guidance and autopilot.

In this work Smooth Second Order Sliding Mode (SSOSM) Control techniques are used to orient the seeker bore sight (collapse of the seeker compensated dynamics is achieved) and to achieve a smooth estimation of target acceleration in finite time. The missile-interceptor *smooth* SSOSM-based robust guidance law (Shtessel et. al., 2007) is integrated into a dual controlled SOSM-based missile autopilot (Tournes et. al., 2006) by inverting to generate smooth flight path angle, angle of attack and pitch rate autopilot commands.

The use of aerodynamic lift increases the divert capability of the missile up to 100%, while the use of divert thrusters provides a fast response to the guidance command. Model uncertainties created by the interactions between the airflow and the thruster-jets are taken into account and compensated for by SOSM-based autopilot. The integrated SOSM guidance-autopilot algorithm is tested via computer simulations against ballistic maneuvering targets.

2. INTERCEPT STRATEGY AND HOSM GUIDANCE

The following state model (Shtessel et. al., 2007) of missile-target engagement kinematics (Fig. 1) is used

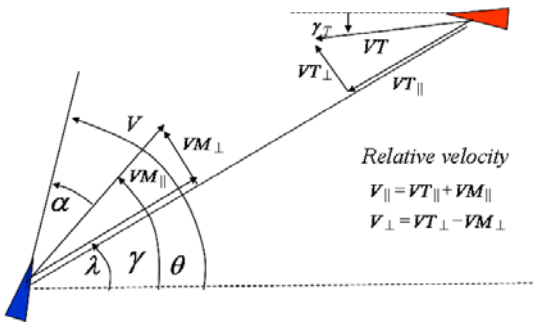

Fig. 1 Intercept geometry

$$\begin{cases} \dot{r} = V_{\parallel}, \\ \dot{V}_{\parallel} = V_{\perp}^2 / r + \Gamma_{\parallel} - \sin(\lambda - \gamma)\Gamma, \\ \dot{\lambda} = V_{\perp}^2 / r, \\ \dot{V}_{\perp} = -V_{\parallel} V_{\perp} / r + \Gamma_{\perp} - \cos(\lambda - \gamma)\Gamma, \end{cases} \quad (1)$$

where r is the range along line-of-sight (LOS), λ is the LOS angle; γ_M is a missile flight path angle, $\dot{\lambda} = \omega_\lambda$ (rad/s) is LOS rate, $V_\perp = r\omega_\lambda$ (m/s) is a transversal component of relative velocity in the reference frame rotating with LOS, Γ is missile normal acceleration, $\Gamma_{||}, \Gamma_\perp$ (disturbances, m/s^2) are projections of bounded target acceleration along and orthogonal to LOS

It is known (Shtessel at. Al. 2005, 2007) that a direct hit can be achieved if

$$V_\perp = c_0\sqrt{r}\,, \tag{2}$$

where $c_0 > 0$ is some constant.

The following guidance strategy can be formulated in terms of SMC: stabilize the system (1) on the manifold

$$\sigma = V_\perp - c_0\sqrt{r} = 0 \tag{3}$$

by means of the normal acceleration command Γ^*. This command is usually followed next by the autopilot.

In this work we propose to use smooth SOSM (SSOSM)-guidance and integrate it into SOSM-based autopilot of a missile interceptor steered by a combination of aerodynamic-lift, sustainer-thrust and center-of-gravity divert thrusters.

3. SMOOTH SECOND ORDER SLIDING MODE CONTROL

3.1 Prescribed Sliding Variable Dynamics

Consider SISO dynamics

$$\dot{\sigma} = g(t) + u\,, \tag{4}$$

which will be further interpreted as dynamics of the sliding variable $\sigma \in \Re^1$ calculated along the system trajectory. The condition $\sigma = 0$ defines the system motion on the sliding surface, $u \in \Re^1$ is a control input that needs to be smooth, and $g(t)$ is an uncertain sufficiently smooth function that is to be cancelled by means of a HOSM observer. The compensated $\sigma-$dynamics in (4) is chosen to have the form

$$\begin{cases} \dot{x}_1 = -\alpha_1 |x_1|^{1/2} sign(x_1) + x_2\,, \\ \dot{x}_2 = -\alpha_2 |x_1|^{1/3} sign(x_1), \qquad \sigma = x_1 \end{cases} \tag{5}$$

Lemma. Let $\alpha_1, \alpha_2 > 0$, then any solution of the system (5) $x_1, x_2 \to 0$ in finite time for any initial conditions.

Proof is omitted for brevity

3.2 Smooth SOSM Disturbance Observer/Differentiator

The sliding variable dynamics (4) is sensitive to the unknown bounded term $g(t)$. Let the variables $\sigma(t)$ and $u(t)$ be available in real time, $g(t)$ be differentiable, so that $\dot{g}(t)$ has a known Lipschitz constant $L > 0$. The control function $u(t)$ is Lebesgue-measurable. Equation (4) is understood in the Filippov sense (see Filippov, 1988), which means in particular that $\sigma(t)$ is an absolutely continuous function defined for any $t \geq 0$.

Consider the HOSM disturbance observer (Levant, 2003):

$$\begin{aligned} \dot{z}_0 &= v_0 + u,\ \ v_0 = -2\cdot L^{1/3}|z_0 - \sigma|^{2/3} sign(z_0 - \sigma) + z_1 \\ \dot{z}_1 &= v_1,\ \ v_1 = -1.5\cdot L^{1/2}|z_1 - v_0|^{1/2} sign(z_1 - v_0) + z_2 \\ \dot{z}_2 &= -1.1\cdot L\cdot sign(z_2 - v_1) \end{aligned} \tag{6}$$

then $z_1 \to g(t)$ in finite time, if the sliding variable σ and control u are measured without noise. If σ and u are measured with some noise bounded by $\varepsilon \geq 0$ and $\varepsilon^{2/3}$ respectively then (Levant, 2003; Shtessel at. al., 2007)

$$|z_1(t) - g(t)| \leq \mu\varepsilon^{2/3}, \quad \mu > 0 \tag{7}$$

3.3 Disturbance cancellation

The following control function smoothly drives $\sigma, \dot{\sigma} \to 0$

$$\begin{cases} u = -z_1 - \alpha_1 |\sigma|^{1/2} \operatorname{sign}(\sigma) + w \\ \dot{w} = -\alpha_2 |\sigma|^{1/3} \operatorname{sign}(\sigma) \end{cases}. \tag{8}$$

If the control law (8) is inserted into the dynamics (4), then the dynamics in eq. (5) result for ideal cancellation. Here z_1 is given by (6) and $\sigma-$ dynamics are given by (4).

Theorem. Let $\alpha_1, \alpha_2 > 0$, $g(t)$ be differentiable, $\dot{g}(t)$ having a known Lipschitz constant $L > 0$. Then the closed-loop system (5) with smooth control (8) and the disturbance observer (6) is finite-time stable.

Proof is omitted for brevity.

Remark 1. The proposed control law (8) can be interpreted as a smooth second order sliding mode (SSOSM) control.

4. SMOOTH SECOND ORDER SLIDING MODE GUIDANCE LAW

From eqs. (1), (3) the σ-dynamics is identified as

$$\dot{\sigma} = g\left(V_{||}(t), V_\perp(t), r(t), \Gamma_\perp(t)\right) - \cos(\lambda - \gamma_M)\Gamma \tag{9}$$

where $g(V_{||}(t), V_\perp(t), r(t), \Gamma_\perp(t)) = -V_{||}V_\perp / r + \Gamma_\perp - c_0 V_{||}/(2\sqrt{r})$,

$$\dot{g}(V_{||}(t), V_\perp(t), r(t), \Gamma_\perp(t)) = -\frac{\left(\dot{V}_{||}V_\perp + V_{||}\dot{V}_\perp\right)r - V_{||}^2 V_\perp}{r^2} + \dot{\Gamma}_\perp - \frac{c_0(2r\dot{V}_{||} - V_{||}^2)}{4r\sqrt{r}}$$

The *smooth* guidance command Γ is to be designed in order to drive $\sigma, \dot{\sigma} \to 0$ in finite time using the SSOSM technique developed in Section 3..

It is worth noting that the singularity point occurs in (9) when intercept by impact happens. However, technically, the intercept by impact ("hit-to-kill") happens when $r \neq 0$ but belongs to the interval $r \in [r_{\min},\ r_{\max}] = [0.1,\ \ 0.25]\,m$ (Garnell and East, 1977; Zarchan, 1998). This fact is due to a certain size of the ballistic target, and a particular intercept value of $r^0 \in [0.1,\ \ 0.25]\,m$, named "zero intercept". Since it is assumed that the function $g(V_{||}(t), V_\perp(t), r(t), \Gamma_\perp(t))$ is differentiable $\forall r \geq r^0$ its derivative has a Lipshitz constant. Assume the following inequalities hold $|\dot{\Gamma}_\perp| \leq \dot{\Gamma}_\perp^{LIM}$, $|\Gamma_\perp| \leq \Gamma_\perp^{LIM}$, $|\Gamma_{||}| \leq \Gamma_{||}^{LIM}$, $|V_\perp(t)| \leq V_\perp^{LIM}$, $V_{||}(0) = M << 0$, $|\sin(\lambda - \gamma_M)| < c_1 < 1$, $|\cos(\lambda - \gamma_M)| < c_2 < 1$, $M \leq V_{||}(t) \leq 0$

in a reasonable flight domain. Then the Lipshitz constant L for $\dot{g}(V_{\|}(t),V_{\perp}(t),r(t),\Gamma_{\perp}(t))$ can be estimated as

$$|\dot{g}| \le \dot{\Gamma}_{\perp}^{LIM} + \frac{\left|\left(\dot{V}_{\|}V_{\perp}+V_{\|}\dot{V}_{\perp}\right)r - V_{\|}^2V_{\perp}\right|}{r^2} + \frac{c_0\left|(2r\dot{V}_{\|}-V_{\|}^2)\right|}{4r\sqrt{r}} \le$$

$$\dot{\Gamma}_{\perp}^{LIM} + \frac{1}{\left(r^0\right)^2}\left[\left(V_{\perp}^{LIM}\right)^3 + 2M^2V_{\perp}^{LIM} + \frac{c_0\sqrt{r^0}}{2}(V_{\perp}^{LIM}+\frac{1}{2}M^2)\right] +$$

$$\frac{1}{r^0}[\left(\Gamma_{\perp}^{LIM}+c_1\Gamma_{\max}\right)V_{\perp}^{LIM} + |M|\left(\Gamma_{\perp}^{LIM}+c_2\Gamma_{\max}\right) +$$

$$\frac{c_0\sqrt{r^0}}{2}(\Gamma_{\perp}^{LIM}+c_1\Gamma_{\max})] = L$$

Since $0 < r^0 << 1$ then $L \approx \dot{\Gamma}_{\perp}^{LIM} + \frac{V_{\perp}^{LIM}}{\left(r^0\right)^2}\left[\left(V_{\perp}^{LIM}\right)^2 + 2M^2\right]$.

Apparently, the smaller zero intercept r^0 yields larger Lipshitz constant L.

Next, assuming the variables $V_{\|}(t), V_{\perp}(t), r(t)$ measured, the target acceleration transversal to LOS can be estimated by the observer (6). This is

$$\begin{aligned}
&\dot{z}_0 = v_0 - \cos(\lambda-\gamma_M)\Gamma - V_{\|}V_{\perp}/r - c_0V_{\|}/(2\sqrt{r}),\\
&v_0 = -2\cdot L^{1/3}\left|z_0-\sigma\right|^{2/3} sign\left(z_0-\sigma\right) + z_1\\
&\dot{z}_1 = v_1,\ v_1 = -1.5\cdot L^{1/2}\left|z_1-v_0\right|^{1/2} sign\left(z_1-v_0\right) + z_2 \qquad (10)\\
&\dot{z}_2 = -1.1\cdot L\cdot sign\left(z_2-v_1\right)\\
&\hat{\Gamma}_{\perp} = z_1
\end{aligned}$$

Apparently, in the absence of input noises we obtain $\hat{\Gamma}_{\perp} = \Gamma_{\perp}$ in finite time. If σ and $\cos(\lambda-\gamma_M)\Gamma + V_{\|}V_{\perp}/r + c_0V_{\|}/(2\sqrt{r})$ are measured with some Lebesgue-measurable noises bounded by $\varepsilon > 0$ and $\varepsilon^{2/3}$ respectively, then (Levant, 2003; Shtessel at. al., 2007)

$$\left|z_1(t) - A_{T,\lambda}\right| \le \mu\varepsilon^{2/3}, \quad \mu > 0 \qquad (11)$$

The prescribed compensated $\sigma-$dynamics that provide finite time convergence is selected in a format (5), and the smooth guidance law is derived in accordance with (8), (10)

$$\begin{cases}
\Gamma^* = \dfrac{1}{\cos(\lambda-\gamma_M)}(-N'\dfrac{V_rV_{\lambda}}{r} + U_d + \hat{\Gamma}_{\perp})\\
U_d = \alpha_1|\sigma|^{1/2} sign\ \sigma + \alpha_2\int|\sigma|^{1/3} sign(\sigma)d\tau - \dfrac{c_0V_{\|}}{2\sqrt{r}}
\end{cases} \qquad (12)$$

5. ANALYSIS OF INTERNAL DYNAMICS

As soon as $\sigma, \dot{\sigma}$ in (3) is reach zero in finite time via the SSOSM guidance law (12) the compensated engagement kinematics (or the forced internal dynamics of the original kinematics in (1)) become

$$\begin{cases}
\dot{r} = V_{\|},\\
\dot{V}_r = c_0^2 + \Gamma_{\|} - \sin(\lambda-\gamma_M)\Gamma^*,\\
\dot{\lambda} = c_0/\sqrt{r},
\end{cases} \qquad (13)$$

Studying eq. (13) we have to find out if there exist a moment $t = t_{\text{int}}$ at which zero-intercept happens, i.e. $|r(t_{\text{int}})| = r^0$.

Assuming $|\Gamma_{\|}| \le \Gamma_{\|}^{LIM}$ the following inequality holds

$$r(t) \le r(0) + Mt + \frac{c_0^2 + \Gamma_{\perp}^{LIM} + c_1\Gamma_{\max}}{2}t^2 \qquad (14)$$

The minimal value of $r(t)$ is identified

$$r(t^*) \le r(0) - \frac{M^2}{2\left(c_0^2 + \Gamma_{\|}^{LIM} + c_1\Gamma_{\max}\right)} \qquad (15)$$

and is achieved at

$$t^* = -\frac{M}{(c_0^2 + \Gamma_{\|}^{LIM} + c_1\Gamma_{\max})} \qquad (16)$$

The parameters $V_r(0) = M < 0$ and $c_0 > 0$ can be selected to meet the condition $|r(t^*)| \le r^0$ that implies the zero-intercept at $t_{\text{int}} \le t^*$ via the SSOSM guidance law (12).

6. PITCH PLANE MATHEMATICAL MODEL OF A DUAL-THRUSTERS CONTROLLED MISSILE

The dynamics of a missile steered by combined effects of divert thrusters and pitch maneuver are given by (Tournes et. al., 2006)

$$\begin{aligned}
\dot{\alpha} = {} & q - Z_{\alpha}(1+\bar{d}_{\alpha})\alpha + \frac{g}{V}\cos(\gamma) - Z_{\delta}(1+\bar{d}_{\delta})\cos(\alpha)\delta\\
& - Z_{\Delta}(1+\bar{d}_{\Delta})\cos(\alpha)\Delta - \cos(\alpha)Z_{\varsigma}\varsigma
\end{aligned} \qquad (17)$$

$$\dot{q} = M_{\alpha}(1+\bar{d}_{\alpha})\alpha + M_qq + M_{\Delta}(1+\bar{d}_{\Delta})\Delta + M_{\delta}(1+\bar{d}_{\delta})\delta + M_{\varsigma}\varsigma \qquad (18)$$

$$\begin{aligned}
\dot{\gamma} = {} & Z_{\alpha}(1+\bar{d}_{\alpha})\alpha - \frac{g}{V}\cos(\gamma) + Z_{\delta}(1+\bar{d}_{\delta})\cos(\alpha)\delta\\
& + Z_{\Delta}(1+\bar{d}_{\Delta})\cos(\alpha)\Delta + \cos(\alpha)Z_{\varsigma}\varsigma
\end{aligned} \qquad (19)$$

where

$$Z_{\alpha} = \frac{\rho SVC_{L_{\alpha}}}{2m},\ Z_{\delta} = \frac{T_{\max\delta}}{mV},\ Z_{\Delta} = \frac{T_{\max\Delta}}{mV},\ Z_{\varsigma} = \frac{T_s}{mV},$$

$$M_{\delta} = \frac{a_{\delta}T_{\max\delta}}{I_{yy}},\ M_{\Delta} = \frac{a_{\Delta}T_{\max\Delta}}{I_{yy}},\ M_{\varsigma} = \frac{a_sT_s}{I_{yy}}$$

α, γ, q are angle-of-attack, flight path angles (*rad*) and pitch rate (*rad s*) respectively; V is longitudinal velocity of a missile (*m/s*). The cumulative disturbances $\bar{d}_{\alpha}, \bar{d}_{\delta}, \bar{d}_{\Delta}$ represent the unknown interactions between attitude thruster jets, divert thruster jets and shockwaves as well as bounded slow-varying perturbations/uncertainties in the stability derivatives. Here it is assumed that $1+\bar{d}_i > 0,\ i = \alpha, \delta, \Delta$.

Actuator dynamics of divert and attitude thrusters and TVC deflection are given by

$$\dot{\Delta} = \frac{1}{\tau_\Delta}(-\Delta + u_\Delta); \quad \dot{\delta} = \frac{1}{\tau_\delta}(-\delta + u_\delta); \quad \dot{\varsigma} = \frac{1}{\tau_\varsigma}(-\varsigma + u_\varsigma) \quad (20)$$

where δ, Δ are normalized attitude and divert thrusters forces; ς is thrust deflection.

Missile acceleration normal to the velocity vector, the commanded output, is related to the flight path angle rate, without account for gravity, as follows:

$$\Gamma = \dot{\gamma} \cdot V \quad (21)$$

The problem is to design a SOSM-based pitch-plane autopilot using Eqs. (17-19) that achieves asymptotic tracking the normal acceleration command $\Gamma^*(t)$ by means of u_i, $i = \delta, \Delta, \varsigma$ in the presence of modeling bounded uncertainties $\bar{d}_\alpha, \bar{d}_\delta, \bar{d}_\Delta$, and also when divert thrusters capability may be insufficient to follow $\Gamma^*(t)$ without the complementary lift created by the attitude maneuver.

The architecture of the Integrated Guidance and Autopilot algorithms steering the interception is represented Fig. 2.

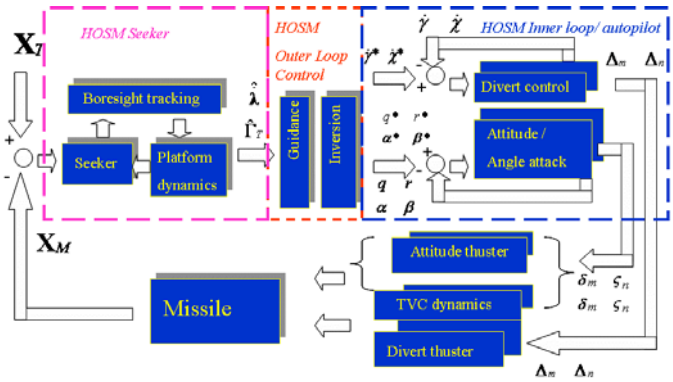

Fig. 2 Guidance and Control Architecture

The seeker (Fig. 2) is supposed to measure LOS λ by pointing to the target. However, its bore site angle $\hat{\lambda}$ differs from the actual LOS λ with an error $\varepsilon = \lambda - \hat{\lambda}$ (Fig. 3).

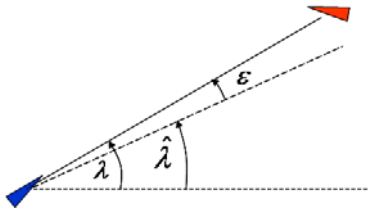

Fig. 3 Seeker geometry

The SSOSM-based controller that is studied in Section 3 is designed to steer $\varepsilon = \lambda - \hat{\lambda} \to 0$.

6. INVERSION/INTEGRATION OF GUIDANCE LAW

First of all, command profiles $\gamma^*, \dot{\gamma}^*, \ddot{\gamma}^*$ are computed in real-time.

$$\dot{\gamma}^*(t) = \frac{\Gamma^*(t)}{V}, \ddot{\gamma}^*(t) = \frac{\dot{\Gamma}^*(t)}{V}, \gamma^*(t) = \frac{1}{V}\int_0^t \Gamma^*(\tau)d\tau, \gamma(0) = \gamma_0 \quad (22)$$

Secondly, the angle of attack command profile α^* and its derivative are computed in real-time assuming full knowledge of stability derivative Z_α and $\dot{\gamma}^*(t)$, while nullifying direct effect of attitude and divert thrusts δ and Δ in (17)-(19)

$$\alpha^* = \begin{cases} \frac{1}{Z_\alpha}[\dot{\gamma}^* + \frac{g}{V}\cos(\gamma^*)], & if \left|\frac{1}{Z_\alpha}[\dot{\gamma}^* + \frac{g}{V}\cos(\gamma^*)]\right| \le \alpha_{\max} \\ \alpha_{\max}, & if \left|\frac{1}{Z_\alpha}[\dot{\gamma}^* + \frac{g}{V}\cos(\gamma^*)]\right| > \alpha_{\max} \\ -\alpha_{\max}, & if \left|\frac{1}{Z_\alpha}[\dot{\gamma}^* + \frac{g}{V}\cos(\gamma^*)]\right| < -\alpha_{\max} \end{cases} \quad (23)$$

$$\dot{\alpha}^* = \begin{cases} \frac{1}{Z_\alpha}[\ddot{\gamma}^* - \frac{g}{V}\dot{\gamma}^*\sin(\gamma^*) - \frac{g\dot{V}}{V^2}\cos(\gamma^*], & if \left|\alpha^*\right| < \alpha_{\max} \\ 0, & otherwise \end{cases} \quad (24)$$

The corresponding pitch rate command q^* is calculated in real-time as the sum of commanded flight path angle rate profile $\dot{\gamma}^*(t)$

$$q^* = \dot{\alpha}^* + \dot{\gamma}^* \quad (25)$$

The pitch rate command profile q^* is supposed to be followed by thruster control u_δ. Clearly $q \to q^*$ implies approximate following $\alpha \to \alpha^*$ while creating a cooperative disturbance term $Z_\alpha \alpha$ in (19), and thus, owing to the robustness of SOSM accuracy following $\alpha \to \alpha^*$ is not required.

Remark 2. It is worth noting that tracking α^* does not imply an accurate tracking of $\dot{\gamma}^*$, since the purpose of the attitude thrusters control is only to generate an aerodynamic maneuver, which in effect is a "cooperative disturbance" that alleviates the divert thrusters control. Next, the difference between γ^* and γ is steered to zero by the divert thrusters control u_Δ in the presence of this cooperative disturbance thereby increasing significantly (up to 100%) the missile overall divert maneuver capability.

7. AUTOPILOT DESIGN

7.1 Second Order Sliding Mode Control Based on Nonlinear Dynamic Sliding Manifold

Equations (17)-(19) (20) have relative degrees equal to two. This calls for SOSM algorithms that are able to drive corresponding sliding variables and their derivatives to zero in finite time.

Remark 3. It is assumed that the missile mathematical model (17)-(19) is of a minimum or slightly non-minimum phase.

Consider SISO sliding variable dynamics

$$\ddot{\sigma} = f(t) + u\,, \qquad \sigma \in \Re^1 \tag{26}$$

where *f(t)* is an uncertain sufficiently smooth function.

Proposition (Shkolnikov et. al., 2005). *Let* $a, b > 0, b > a$, $f(t)$ *be differentiable,* $\bar{\rho} > 0$ *be sufficiently large and a control law is defined*

$$u = -\bar{\rho} \cdot sign(J)\,, \tag{27}$$

*then t*he close-loop system (26), (27) is finite time stable ($\sigma, \dot{\sigma} \to 0$ in finite time) with a nonlinear dynamic sliding manifold (NDSM) *J* defined as

$$\begin{cases} \dot{\chi} = a\left|\sigma\right|^{0.5} sign(\sigma) - b\left|\chi + \sigma\right|^{0.5} sign(\chi + \sigma), \\ J = \chi + \sigma. \end{cases} \tag{28}$$

Remark. 4. The SOSM control law (27), (28), called SOSM/NDSM control, does not require σ -differentiation. In order to achieve a given frequency of control switching, the nonlinear dynamic sliding variable J can be mixed with a dither signal of a given frequency. In this case the control function (27) will be pulse-width modulated. A graceful degradation of stabilization accuracy is expected due to reduction of control switching frequency.

7.2 Design of Pitch Rate Control via Attitude Thrusters

The pitch rate dynamics are derived based on eqs. (17), (18), (20) with thrust vectoring terms containing ς removed, since thrust vectoring is not used altogether with attitude thrusters.

Following the SOSM/NDSM control design technique the pitch-rate sliding variable is introduced

$$\sigma_q = \varepsilon_q + \varpi \int_0^t \varepsilon_q(\tau) d\tau, \quad \varepsilon_q = q^* - q, \quad \varpi = 50\, rad/\sec \tag{29}$$

Eq. (29) shows that, once the sliding surface $\sigma_q = 0$ is achieved at the finite time, the pitch rate tracking error ε_q converges to zero asymptotically according to the eigenvalue of $\sigma_q = 0$. Differentiating twice eq. (29) gives

$$\ddot{\sigma}_q = f_q(t) - b_\delta u_\delta \tag{30}$$

where

$$\begin{cases} f_q(t) = \ddot{q}^* + \varpi \dot{q}^* - M_\alpha(1 + \bar{d}_\alpha)\dot{\alpha} - (M_q + \varpi)\dot{q} - \\ M_\Delta(1 + \bar{d}_\Delta)\dot{\Delta} + \dfrac{M_\delta d_\delta}{\tau_\delta}(1 + \bar{d}_\delta)\delta; \quad b_\delta = \dfrac{M_\delta(1 + \bar{d}_\delta)}{\tau_\delta} \end{cases}$$

One can easily show that, the disturbance $f_q(t)$ is bounded in an operational domain $\Omega_q : \left|f_q(t)\right| \le L_q$. Since it is assumed that $\left|\bar{d}_\delta\right| < 1, M_\delta > 0$ then $b_\delta > 0, b'_\delta < b_\delta < b''_\delta$ and the SOSM/NDSM based control in (27), (28) can be employed for stabilizing σ_q and its derivative $\dot{\sigma}_q$ at zero in finite time. Corresponding SOSM/NDSM-based attitude thrust controller is given by

$$\begin{cases} \dot{\chi}_q = \xi_q \left|\sigma_q\right|^{0.5} sign(\sigma_q) - \eta_q \left|\chi_q + \sigma_q\right|^{0.5} sign(\chi_q + \sigma_q) \\ J_q = \chi_q + \sigma_q, \quad u_\delta = -\bar{\rho}_q \cdot sign(J_q) \end{cases} \tag{31}$$

7.3 Design of the Angle of Attack Thrust Vectoring Autopilot

The angle of attack dynamics are derived base on eqs. (17), (20). It is worth noting that, in practice $\max\left|Z_\delta \delta + Z_\Delta \Delta\right| << \max\left|q\right|, \quad \max\left|M_\delta\right| >> \max\left|M_\Delta\right|$.

It means that the missile angle of attack α is mostly governed by the pitch rate q, which itself is controlled by the attitude thrusters-force δ. The sliding surface σ_α is defined

$$\sigma_\alpha = \varepsilon_\alpha + \varpi \int_0^t \varepsilon_\alpha d\tau, \quad \varepsilon_\alpha = \alpha^* - \alpha, \quad \varpi = 20\, rad/s \tag{32}$$

Differentiating (32) twice with respect to time gives

$$\ddot{\sigma}_\alpha = f_\alpha(t) - b_\varsigma u_\varsigma \tag{33}$$

Where one can show that similar to Eq. (30) $f_\alpha(t)$ is a bounded variable while $b_\varsigma = M_\varsigma / \tau_\varsigma$, and the angle of attack thrust vectoring controller is given by

$$\begin{cases} \dot{\chi}_\alpha = \xi_\alpha \left|\sigma_\alpha\right|^{0.5} sign(\sigma_\alpha) - \eta_\alpha \left|\chi_\alpha + \sigma_\alpha\right|^{0.5} sign(\chi_\alpha + \sigma_\alpha) \\ J_\alpha = \chi_\alpha + \sigma_\alpha, \quad u_\varsigma = -\bar{\rho}_\alpha \cdot sign(J_\alpha) \end{cases} \tag{34}$$

7.4 Design of flight path Autopilot

The flight path angle input-output dynamics are derived based on Eqs. (19), (20) and are controlled using SOSM/NDSM-based attitude control (27), (28). Similarly the divert (flight path angle) thrust sliding variable is introduced

$$\sigma_\gamma = \varepsilon_\gamma + \omega \int_0^t \varepsilon_\gamma(\tau) d\tau, \quad \varepsilon_\gamma = \gamma^* - \gamma, \quad \omega = 50\, rad/\sec \tag{35}$$

Equation (35) shows that, once the sliding surface $\sigma_\gamma = 0$ is achieved in finite time, $\varepsilon_\gamma \to 0$ asymptotically.

Differentiating σ_γ in (35) twice, the following σ_γ input-output dynamics are derived

$$\ddot{\sigma}_\gamma = f_\gamma(t) - b_\Delta u_\Delta \tag{36}$$

where

$$\begin{cases} f_\gamma(t) = \ddot{\gamma}^* + \omega \dot{\gamma}^* + [Z_\alpha(1 + \bar{d}_\alpha) - Z_\delta(1 + \bar{d}_\delta)\sin(\alpha)\delta - \\ Z_\Delta(1 + \bar{d}_\Delta)\sin(\alpha)\Delta]\dot{\alpha} + (\dfrac{g}{V}\sin(\gamma) - \omega)\dot{\gamma} + Z_\delta(1 + \bar{d}_\delta)\cos(\alpha)\dot{\delta} - \\ \dfrac{Z_\Delta(1 + \bar{d}_\Delta)\cos(\alpha)}{\tau_\Delta}\Delta, \quad b_\Delta = \dfrac{Z_\Delta(1 + \bar{d}_\Delta)\cos(\alpha)}{\tau_\Delta} \end{cases}$$

It is assumed that the disturbance $f_\gamma(t)$ is bounded in an operational domain $\Omega_\gamma : \left|f_\gamma(t)\right| \le L_\gamma$, as well as $\left|\bar{d}_\Delta\right| < 1$, $Z_\Delta > 0$ and $\left|\alpha\right| \le 0.5$, then $b_\Delta > 0$, $b'_\Delta < b_\Delta < b''_\Delta$, and the SOSM/NDSM-based divert thrust controller is designed similar to the one in eqs. (27), (28)

$$\begin{cases} \dot{\chi}_\gamma = \xi_\gamma \left|\sigma_\gamma\right|^{0.5} sign(\sigma_\gamma) - \eta_\gamma \left|\chi_\gamma + \sigma_\gamma\right|^{0.5} sign(\chi_\gamma + \sigma_\gamma) \\ J_\gamma = \chi_\gamma + \sigma_\gamma, \quad u_\Delta = -\bar{\rho}_\gamma \cdot sign(J_\gamma) \end{cases} \tag{37}$$

8. SIMULATIONS

Simulation results of a dual-thrusters and thrust vectoring controlled missile interceptor against SS-27-like maneuvering target using the designed integrated SOSM-based guidance-

autopilot are presented in Figures 4-9. The planar engagement that ends up in a direct hit is illustrated in Fig. 4. Small estimation errors of LOS and LOS rates characterize a high accuracy performance of HOSM observers in presence of a significant measurement noise. High accuracy estimation of target normal acceleration $\Gamma_{\perp}$ via compensated seeker and via HOSM observer are shown in Fig 5.

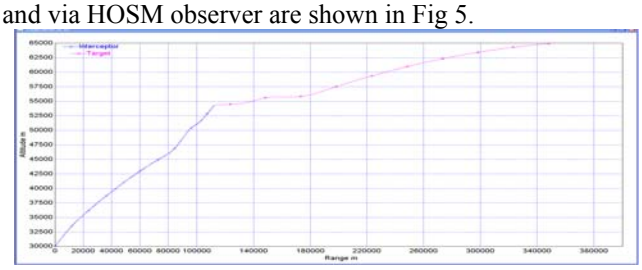

Fig. 4 Incoming intercept (down range versus cross range)

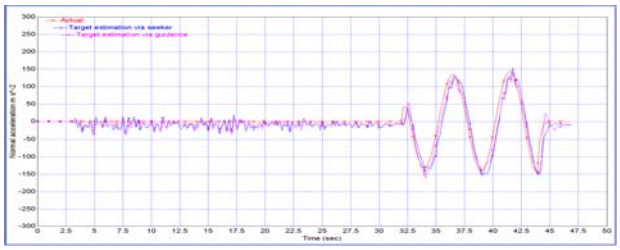

Fig. 5 Estimation of target normal acceleration

The interceptor normal acceleration Γ closely mimics $\Gamma_{\perp}$ (fig 6) providing for a small acceleration advantage. The performance of the integrated SOSM guidance/autopilot is illustrated by a very accurate flight path angle (Fig. 7) and pitch rate tracking (fig. 8). Fig. 9 shows typical multiplicative normalized disturbance plot. The results are achieved by TVC and attitude thruster's control.

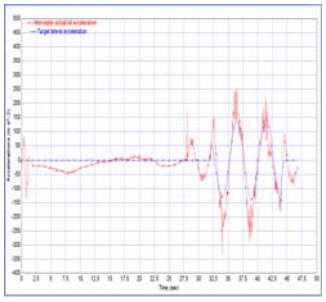

Fig. 6 Comparison of interceptor and target wave maneuvers

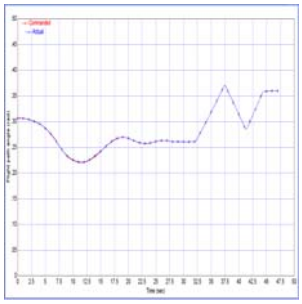

Fig. 7 Flight path angle tracking

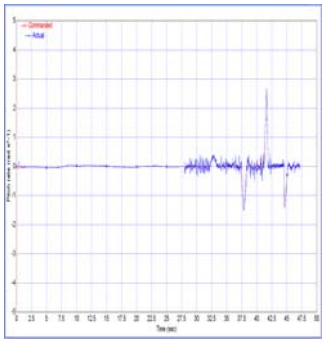

Fig. 8 Pitch rate tracking performance

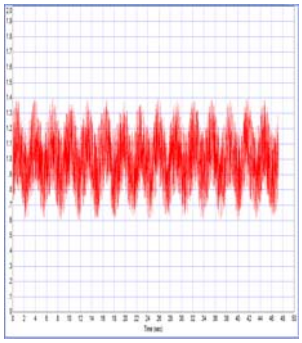

Fig. 9 Typical normalized multiplicative disturbance

9. CONCLUSIONS

Novel smooth second-order sliding mode (SSOSM) control is studied and used for the missile-interceptor guidance design against a target performing evasive maneuvers. HOSM estimator reconstructs the target normal acceleration. The missile autopilot is based on Nonlinear Dynamic Sliding Manifold technique. Integrated SOSM-based guidance/autopilot performance was studied via computer simulations. The excellent results have been obtained against stressing sine wave target maneuvers. Not withstanding the rapid pace of the maneuvers the algorithm achieves extreme estimation and intercept accuracy. The excellent simulation results were obtained in the presence of very significant model uncertainties and measurement noise.

REFERENCES

Garnell P. and East D. J. (1977). Guided Weapon Control Systems, Oxford: Pergamon Press.

P. Zarchan (1998). Tactical and Strategic Missile Guidance. 176, Progress in Astronautics and Aeronautics, AIAA Publications.

Edwards C., and Spurgeon S. (1998). *Sliding Mode Control,* Taylor & Francis, Bristol, PA.

Idan, M., Shima, T. and Golan, O., (2007), "Sliding Mode Integrated Autopilot-Guidance for Dual Control Missiles" *AIAA Journal of Guidance, Control, and Dynamics*, Vol. 30, No. 4, pp. 1081-1089.

Moon J., and Kim Y. (2000). Design of missile guidance law via variable structure control, *Proceedings of AIAA Guidance, Navigation and Control Conference*, Denver, CO, Paper AIAA-2000-4068

Shkolnikov I., Shtessel Y., and Lianos D. (2001). Integrated Guidance-Control System of a Homing Interceptor: Sliding Mode Approach, *Proceedings of AIAA Guidance, Navigation, and Control Conference*, AIAA Paper 2001-4218.

Levant A. (2003). Higher-order sliding modes, differentiation and output-feedback control, *International Journal of Control*, Vol. 76, No. 9/10, pp. 924-941.

Shtessel Y., Shkolnikov I., and Levant A., (2007). Smooth Second Order Sliding Modes: Missile Guidance Application, *Automatica*, Vol. 43, No.8, pp. 1470-1476.

Shtessel Y., Shkolnikov I., and Levant, A. (2005). Missile Interceptor Guidance and Control Using Second Order Sliding Modes, *Proceedings of IFAC World Congress*, Prague, Czech Republic.

Tournes, C. Shtessel, Y. and Shkolnikov, I. (2006), Autopilot for Missiles Steered by Aerodynamic Lift and Divert Thrusters Using Nonlinear Dynamic Sliding Manifolds, *AIAA Journal on Guidance, Control, and Dynamics,* Vol. 29, No. 3, pp. 617-625.

Filippov A. F. (1988). Differential Equations with Discontinuous Right-Hand Side, Kluwer, Dordrecht, Netherlands.

Shkolnikov I., Shtessel Y., and Lianos D. (2005). The effect of sliding mode observers in the homing guidance loop, *IMechE Journal on Aerospace Engineering*, *Part G, 219*, 2, pp. 103-111.